Digest Journal of Nanomaterials and Biostructures Vol. 7, No. 2, April - June 2012, p. 823 - 832

INVESTIGATION OF HYBRID METHACRYLATE BASED STRUCTURES OBTAINED BY POLYMERIZATION WITH FEMTOSECOND LASER PULSES

A. MATEI[a,b*], M. ZAMFIRESCU[b], M. DINESCU[b], E.C. BURUIANA[a], T. BURUIANA[a], A. LUNGU[c], C. MUSTACIOSU[d]

[a]*Petru Poni Institute of Macromolecular Chemistry, Grigore Ghica Voda 41A, 6600 Iasi, Romania*

[b]*National Institute for Lasers, Plasma and Radiation Physics, Atomistilor 409, 77125 Bucharest-Magurele, Romania*

[c]*Advanced Polymer Materials Group, Faculty of Applied Chemistry and Materials Science, University "POLITEHNICA" of Bucharest, Calea Victoriei 149, 010072, Bucharest, Romania*

[d]*Department of Environmental and Life Physics, National Institute for Physics and Nuclear Engineering 'Horia Hulubei', Bucharest, Romania*

In this work we report on the polymerization via direct laser writing using ultrashort laser pulses of a hybrid methacrylate based on silane derivatives. For the preparation of 2D and 3D structures the organic-inorganic material was laser processed alone or in a monomer mixture. The chemical structure, elemental composition of the monomers and of the processed polymeric structures, as well as the morphology of the fabricated systems were investigated, with the aim to develop novel materials for further application in tissue engineering and biomedical implants.

(Received April 3, 2012; Accepted June 14, 2012)

1. Introduction

In the last years, the synthesis of hybrid organic-inorganic nanomaterials has proved to be a topic with a very promising future. Organically modified silicates, known as ormosils are hybrid monomers with strong covalent bonding between the organic group and the inorganic one. The materials with tailored properties lead to a tremendous research activity exploring the development of novel biomaterials as scaffolds in tissue engineering and regenerative medicine [1, 2], coatings with a wide range of pharmaceutical [3], biomedical implants [4, 5] and sensor applications [6-8]. The ormosils can be used as waveguides and photonic components [9-11] as well as protective coatings [7, 12] due to their good optical and mechanical properties as well as thermal stability [13].

In order to successfully use an ormosil for tissue engineering, there are few requirements to be fulfilled. The material has to be biocompatible, to have a porous structure and it has to be easily structured [14]. The artificial designed scaffold has to simulate the natural cellular environment of the living body [15]. The geometry and topography of the polymeric matrix have a significant influence in the cells orientation, alignment and the first steps for tissue formation [1, 16]. If for a bidimensional structure the typical cells growth model is in a single layer, for a tissue, with 3D configuration and different cell types present, a 3D system is needed [9]. The scaffold configuration has to vary with respect to the cells involved; for example, the pore size required for a fibroblast cell is about 10 μm, which is 10 times lower than for an osteocyte, as mentioned in

*Corresponding author: andreeapurice@nipne.ro

Ref. 17 and Ref. 6 heir in. For this reason the method of producing the scaffold should allow easily setting and configuration.

Laser based techniques have proved to be an attractive alternative to the conventional methods (e.g. gas foaming [17]) due to the number of advantages it has to offer over the conventional processes, such as being a clean technique that can generate structures with well controlled architecture; the laser is an external energy source needed for polymerization and by this way no contamination is introduced. Selective laser sintering uses a high power laser (e.g. a CO_2) to produce solid 3D structures starting from powder materials [18]. The main disadvantage of laser sintering is that most of the materials suitable for sintering are not biocompatible. Stereolithography uses UV lasers for the polymerization of photosensitive materials. Polymerization takes place up to a few micrometers below the surface [19]. In-plane scanning of the sample produces 2D structures, while 3D scaffolds can be built by multiple scanning, layer by layer, each time on fresh photosensitive material, the layers attaching on the previous ones.

A very appealing method for producing 3D biocompatible scaffolds with high resolution (under the diffraction limit) [21] is direct laser write (DLW) with ultrashort pulses [9, 22]. By focusing the beam of an infrared laser with ultrashort pulses into the volume of a photosensitive material, the photopolymerization process takes place just in the center of the focus spot. The dominant mechanism involved in the polymerization by femtoseconds is avalanche absorption which is seeded by multi photon absorption process [22]. By moving the laser beam inside the volume of the transparent material, the photopolymerization is initiated by two photon absorption and 3D structures can be designed and obtained. Hybrid materials photo processed by femtosecond laser pulses can find other applications in drug delivery [23-25] as well as implants for biomedicine and photonic crystals [15, 23, 26, 27].

In this study we investigated the chemical properties and the morphology of structures obtained by direct laser writing (DLW) that allow producing scaffolds with micrometer resolution for applications in tissue engineering. Previously, the biocompatibility tests performed evidenced that the hybrid monomer is not cytotoxic [13].

2. Materials and methods

2.1 Materials

The chemical structure of the triethoxysilane based methacrylate is presented in Fig. 1.a. N,N'-(methacryloyloxyethyl triehtoxy silyl propyl carbamoyl-oxyhexyl)-urea (SIM-3) is the monomer used in our study for laser photostructuring experiments, by femtosecond laser pulses. This monomer has been polymerized alone or by combining it with a co-monomer consisting in a dimethacrylate oligomer with urethane groups in its structure (Fig 1.b).

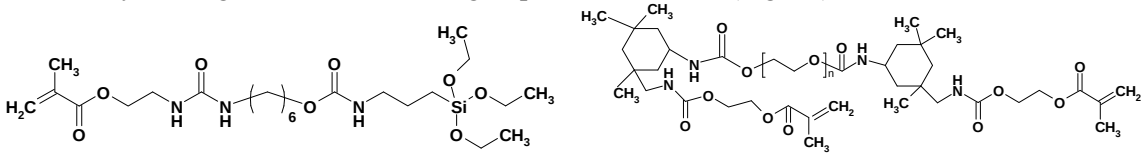

(a) (b)

Fig. 1. The chemical structure of (a) N,N'-(methacryloyloxyethyl triehtoxy silyl propyl carbamoyloxyhexyl)-ureea (SIM-3) and (b) oligourethane dimethacrylate (UDA)

2.2 Scaffold Preparation

Solutions of monomer and photoinitiator in tetrahydrofuran were prepared and deposited on glass substrate (by drop casting method) as described in [28, 29]. For the experiments where the urethane dimethacrylate was used as co-monomer, the ratio SIM-3:UDA was 3:1. Commercial Irgacure 369 was selected as efficient photoinitiator. A Direct Laser Writing workstation coupled with an amplified femtosecond laser Clark CPA-2010 was the setup for the polymerization

experiments. The Ti:Sapphire laser emits ultrashort pulses of 200 fs at wavelength of 775 nm. The repetition rate was 2 kHz.

The sample, consisting in the monomeric gel distributed in a thin and uniform layer on a glass substrate, was maintained fixed. The surface was scanned by a laser scanning head with galvanic mirrors. The laser beam was focused on the sample by a f-theta lens of 100 mm focal distance, providing a focal spot diameter of 35 μm. Areas up to 5x5 mm^2 were scanned and photo-processed by ultrashort laser pulses and structures of lines and grids with different spacing have been photopolymerized. The laser processing parameters were optimized for the best results in terms of structures uniformity, smoothness of the structures, defects free. Therefore, the laser power was in the range 5-10 mW, leading to a fluence of about 0.2-0.5 J/cm^2 and the laser beam scanning velocity was in the range 1-3 mm/s.

2.3 Analysis

The structure and purity of the monomers was checked by ^{1}H NMR spectroscopy and Fourier Transform Infrared spectroscopy. The temperature stability of the hybrid polymers was investigated by thermal analysis (Thermogravimetric methods (TGA/DTG)) with a TA Q500 derivatograph, by heating the sample (2 mg) with 10^{o}C/ minute up to 800°C, in N_2 atmosphere (90 ml/ minute gas flow). The thermal analyses were performed on samples polymerized with a nanosecond Nd: YAG laser, working at 266 nm, and 10 Hz repetition rate. The laser energy and laser spot were 15 mJ and 0.5 cm^2 respectively.

The elemental composition of the structures obtained by DLW with femtosecond laser pulses was determined by X-ray photoelectron spectroscopy (XPS). The XPS spectra were recorded on the Thermo Scientific KAlpha equipment, fully integrated, with an aluminum anode monochromatic source. The surface morphology of the polymerized structures was investigated by optical microscopy, scanning electron microscopy (SEM) and atomic force microscopy (AFM).

L929 mouse fibroblasts cells were grown on the photo structured scaffolds in order to study the cells attachment and proliferation. Cells were grown in medium MEM (Minimal Essential Medium), produced by Biochrom, 1% penicilin-streptomicin, L-glutamine and 10% heat inactivated fetal bovine serum and they were kept in an incubator at 37°C, 5% CO_2.

We used phalloidin to mark actin cytoskeleton and hoecst to identify the nuclei. For cells observation an Olympus microscope IX 71 was used. The pictures were taken using a Moticam 2300, 3 Mp camera attached to the microscope (Motic Images Plus 2.0 software).

3. Results and discussions

Fig. 2 presents the ^{1}H NMR spectrum of N,N'-(methacryloyloxyethyl triehtoxy silyl propyl carbamoyl-oxyhexyl)-urea (SIM-3), in which can be identified the characteristic signals for olefinic protons in trans/cis configuration (6.1 and 5.6 ppm), urea protons (5.1 and 4.9 ppm), methylene protons of ester-urethane (4.2 ppm) and ester functions (4.0 ppm), protons of siloxane (3.8 and 3.7 ppm), or protons bonded to urea (3.5 ppm) and urethane (3.15 ppm) groups. The other signals belong to methyl protons of methacrylate (1.8 ppm), methyl protons of hexyl and propyl (1.2-1.6 ppm), and CH_2–Si protons (0.6 ppm). The FTIR spectrum of SIM-3 (Fig. 3) shows the specific absorption bands of the urea and urethane NH group (3357 cm^{-1}), C-H group (2973, 2927 cm^{-1}), carbonyl group (1720 cm^{-1}), methacrylate function (1639 cm^{-1}), amida II (1566 cm^{-1}), and Si-O moiety (1079 cm-1).

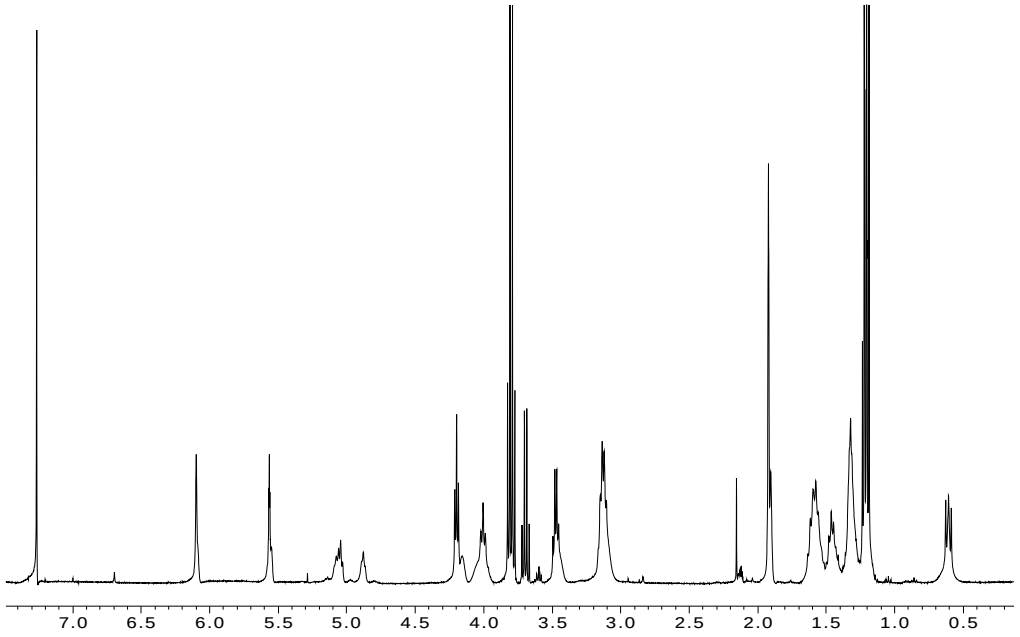

Fig. 2. ^{1}H NMR spectrum of N,N'-(methacryloyloxyethyl triehtoxy silyl propyl carbamoyloxyhexyl)-urea (SIM-3) in $CDCl_3$

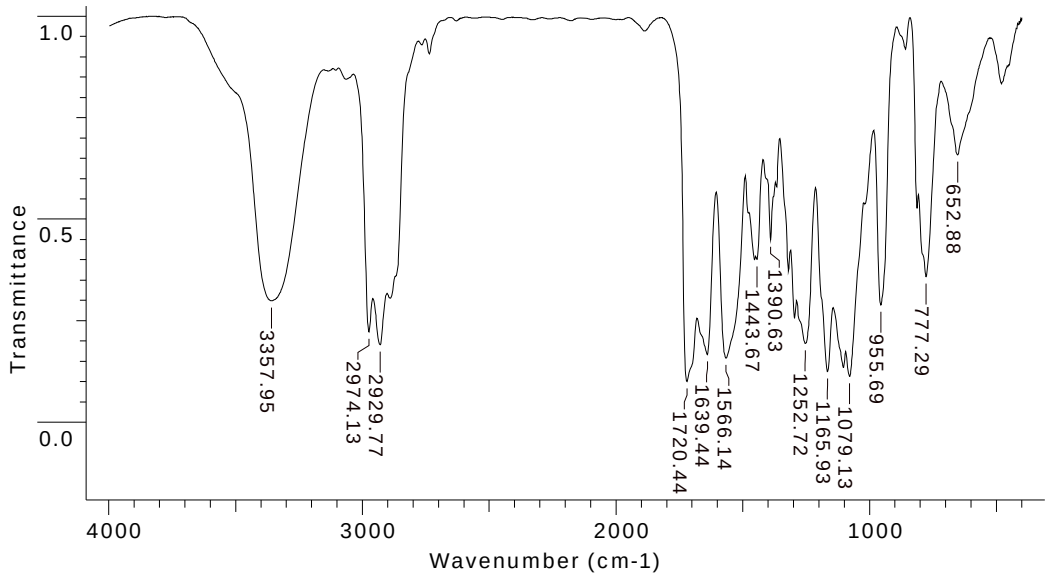

Fig. 3. FTIR spectrum of N,N'-(methacryloyloxyethyl triehtoxy silyl propyl carbamoyloxyhexyl)-urea (SIM-3)

SIM-3 was tested alone or in combination with an urethane dimethacrylate (UDA) that contains the poly(ethylene oxide) soft segment as spacer between the photopolymerizable groups. Fig. 4 presents the ^{1}H NMR spectrum for UDA. The signals at 0.88-1.70 ppm correspond to the isophorone cycle protons and those at 1.87 ppm are attributed to methyl protons bonded to the polymerizing groups. Methylene protons of urethane groups are visible by 3.3 ppm signal, methylene protons of poly(ethylene oxide) by 3.55 ppm, methylene protons of urethane groups by 3.6 ppm and methylene protons of ester group by 4.20 ppm signal. The other signals belong to unsaturated acrylate protons (5.65 and 6.03 ppm) and urethane protons (7.19 and 7.80 ppm).

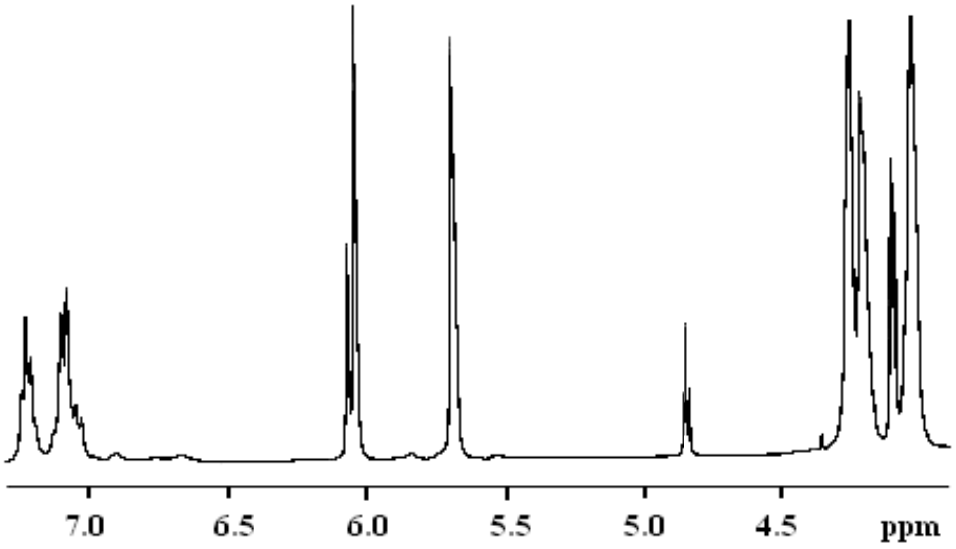

Fig. 4. ^{1}H NMR spectrum of urethane dimethacrylate (UDA) in $CDCl_3$

The TGA and DTG curves for the hybrid polymers are given in Fig. 5 (a, b).

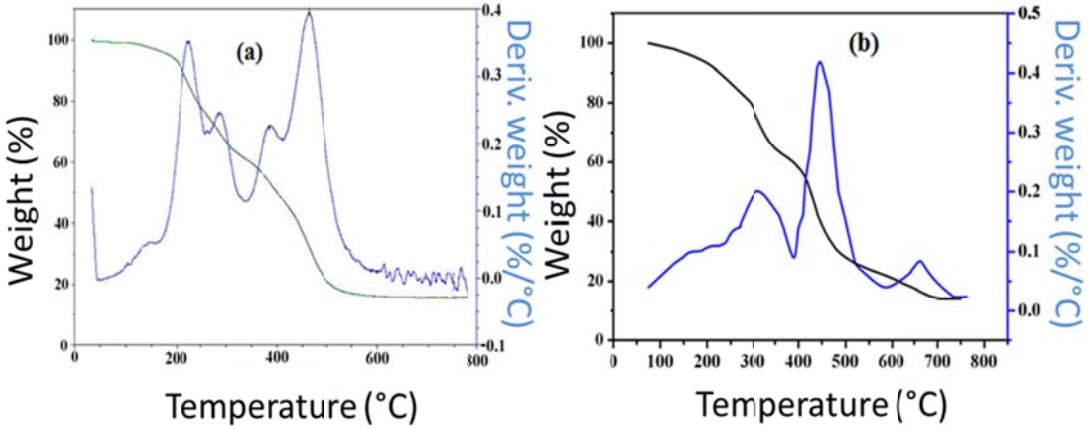

Fig. 5. TGA and DTG curves for the polymerized SIM-3 (a) and SIM-3:UDA (b)

Analyzing the thermal data it can be noticed that the decomposition of hybrid homopolymer (a) showed four degradation stages with a total loss of mass around 84 wt% at around 580°C. The first stage of thermal decomposition (T_{onset}) starts at 150°C, and is related to the organic fraction of the hybrid polymer. The temperature at which 10 wt% of the sample weight has been lost, namely $T_{d,10\%}$ was of 225°C and the final temperature (T_{endset}) was of 250°C. At this point the loss of mass was estimated to 25 wt%. The second degradation stage begins at 250°C (weight loss of 10 wt%) and it can be ascribed to further degradation of the organic polymer chain. After 380°C it can be assumed that a complex decomposition of the polymer occurred. The observed experimental residue of 12 % is in reasonable agreement with the calculated value for the silica content of the formed silsesquioxane structure. In the case of hybrid copolymer resulted from the mixture SIM-3:UDA (b) four stages of degradation process were found, the first stage (100-235°C) corresponding to the solvent (5% weight loss). The second stage (230-380°C) is usually attributed to the polymer chain breakdown (35% weight loss), while the third (40% weight loss) can be related to the breaking of the organic component. In the final stage (over 540°C) a weight loss of 5% and 12% residue content was registered. It can be observed that in the range 100-300°C the hybrid homopolymer seems to be more stable than the hybrid copolymer; we can then conclude

that autoclaving is a suitable sterilization method in cells culture experiments for both samples (SIM-3 and SIM-3:UDA).

XPS analysis is employed to examine the surface composition of hybrid polymers obtained by polymerization of SIM-3 and the monomer mixture SIM-3:UDA at initial monomer ratio of 3:1, using the laser incident power of 7.5 mW and the scanning velocity of 1 mm/s. Fig. 6 (a, b) contains the XPS survey spectra of polymerized SIM-3 and SIM-3:UDA, both spectra revealing the characteristic peaks corresponding to carbon atoms in the aliphatic chain with binding energies of 284.7 eV/SIM-3 or 284.7 eV/SIM-3:UDA, nitrogen atoms (398.42 eV/SIM-3; 399.09 eV/SIM-3:UDA), oxygen atoms (530.94 eV/SIM-3; 531.76 eV/SIM-3:UDA) and silicon atoms (102.24 eV/SIM-3; 101.57 eV/SIM-3:UDA). In the spectrum of SIM-3 the relative atomic concentrations of carbon, nitrogen, oxygen and silicon elements are 21.8 %, 64.58 %, 10.38 % and 3.24 % respectively. In the spectra of the copolymer based SIM-3:UDA, the atomic concentration of oxygen increases to 24.03 %, while the atomic concentration of nitrogen decreased to 8.3 %. This result supports the fact that the amount of urethane and urea groups at the surface of the latter decreased from SIM-3 to SIM-3:UDA.

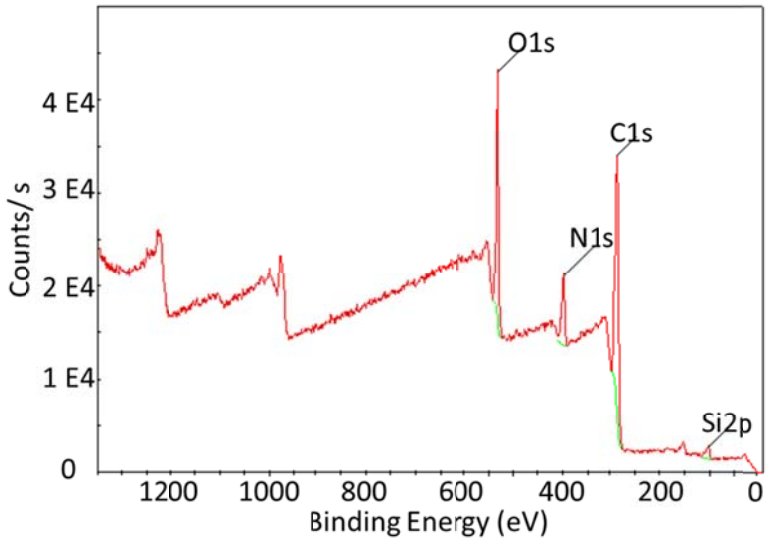

(a)

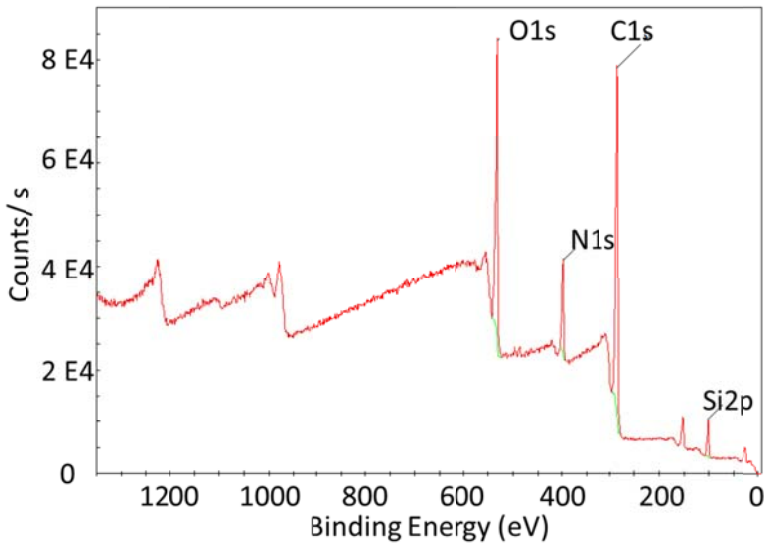

(b)

Fig. 6. General XPS spectra for the polymerized SIM-3 (a) and polymerized SIM-3:UDA (b)

3D structures of polymerized SIM-3 with 2 layers are presented in Fig. 7. They have been built as the result of double laser scans, with a laser power of 7.5 mW and raster velocity of 1 mm/s. The spacing between the lines is 100 μm and the processed area is 5x5 mm^2. There are 2 layers grids; for the first one, the top layer is shifted with 50 μm on one axis, and for the second, the layers are aligned on top of each other. A SEM micrograph is also presented for a better view of the polymer surface (Fig. 8). The polymer is smooth, with relatively few defects on the surface. For a single layer structure, processed in the same conditions as above, the thickness and the height of the lines are both around 10 μm, as it was identified by AFM studies (Fig. 9).

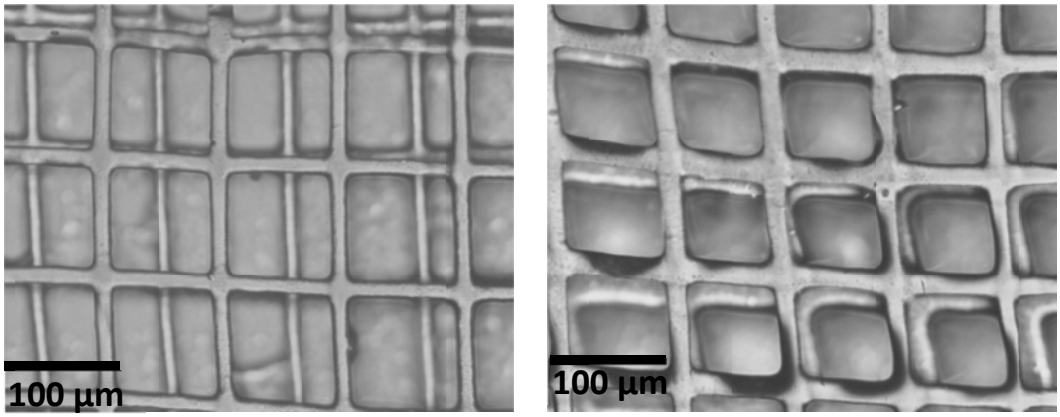

Fig. 7. Optical images on 2 layers structures.

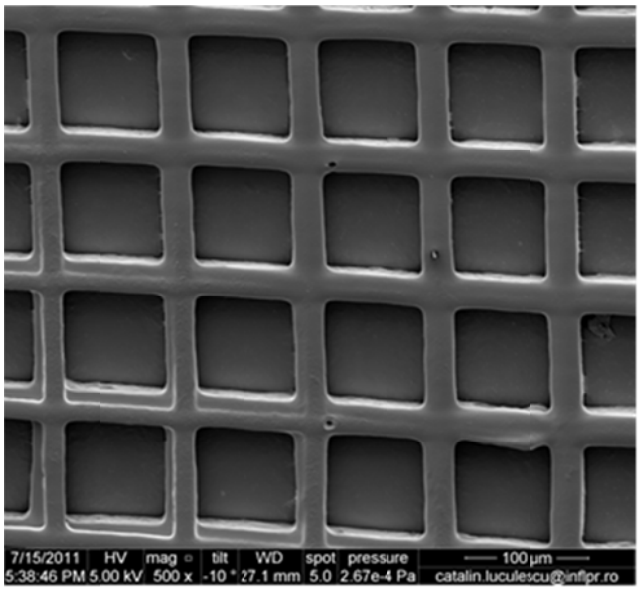

Fig. 8. SEM image on the two layers structure from fig. 7

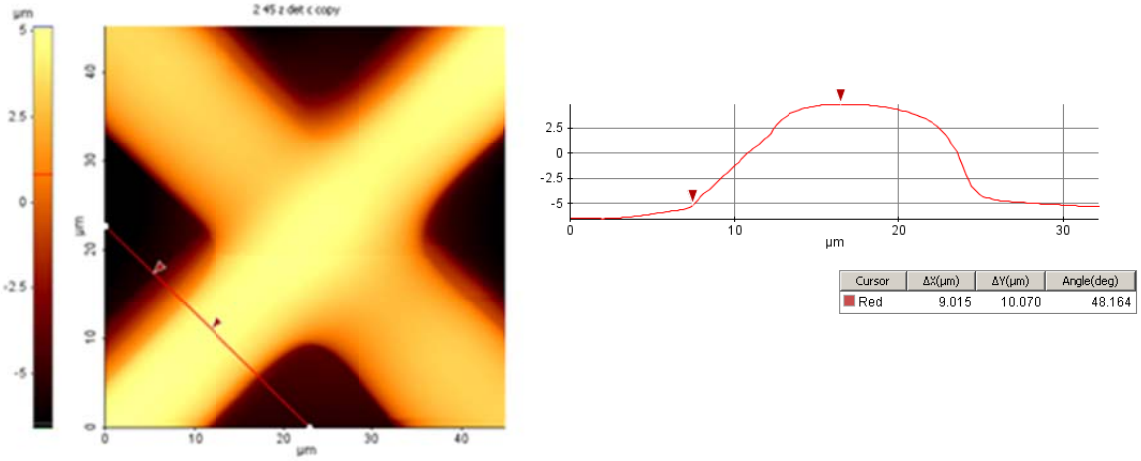

Fig. 9. AFM image on a SIM-3 single layer grid.

The biocompatibility of SIM-3 polymerized samples was investigated using the agar diffusion test (according to ISO/EN 10993-5) [30] and it showed the non-cytotoxicity of the materials [13]. The fibroblast cells attach and proliferate on polymeric scaffolds. An example is presented in the next figure for a grid obtained on a glass substrate, with 100 µm repetition distance. As it can be seen, the cells mainly adhere and remain on the polymeric structures (Fig. 10).

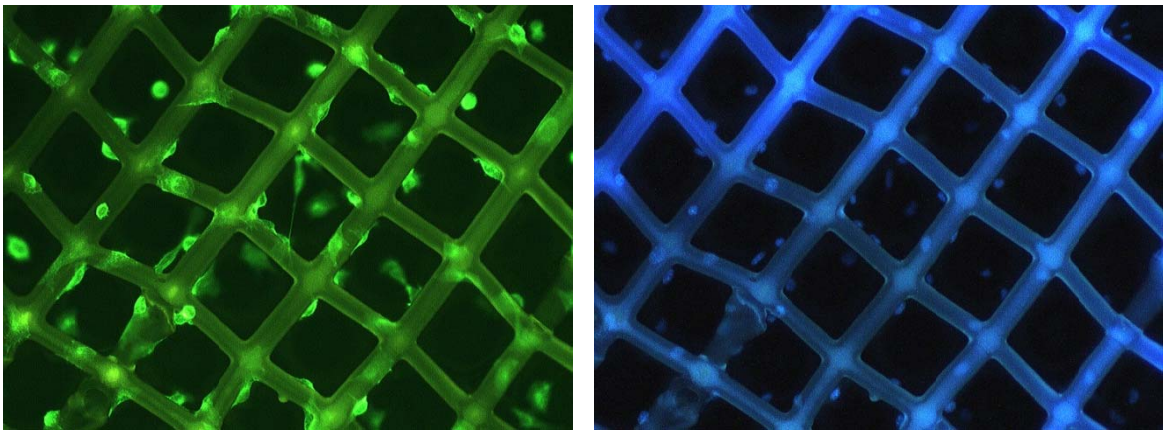

(a) (b)

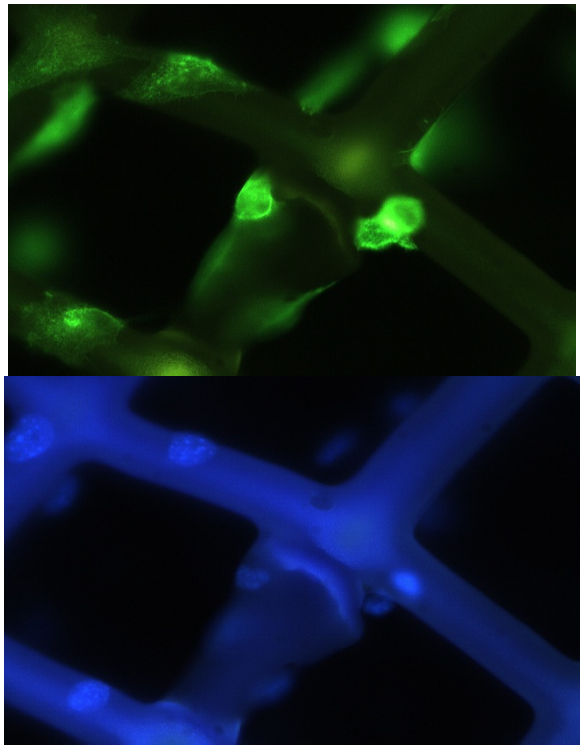

(c) (d)

Fig. 10. Fibroblast cells grown on a polymeric grid with 100 µm distance between lines. Marked actin filaments (a, c) and nuclei (b, d) (4 days) for two different magnifications

By using phalloidin staining, it can be observed (Fig 10 (a, c)), that the cells are stretched on the grid surface, establishing intercellular connections with a tendency to cover the scaffold, the chemistry of the organic-inorganic hybrid materials and the surface topography being proper for the cells growth and proliferation.

4. Conclusions

2D and 3D polymeric structures were obtained by direct laser writing with femtosecond pulses, for SIM-3 alone or in combination with the urethane diacrylate oligomer (UDA). Large areas can be fabricated with a time effective technique. The biological tests proved the biocompatible character of the polymers, with prospects for bio applications.

Acknowledgements

Two authors (A.M. and T.B.) acknowledge the financial support of European Social Fund – „Cristofor I. Simionescu" Postdoctoral Fellowship Programme (ID POSDRU/89/1.5/ S/55216), Sectoral Operational Programme Human Resources Development 2007 – 2013.

References

[1] L.E.Sima, S.M. Petrescu, E. C. Buruiana, T. Buruiana, A. Matei, G. Epurescu, M. Zamfirescu, A. Moldovan, M. Dinescu, J Tiss Eng Reg Med, DOI: 10.1002/term.507 (2011).
[2] G. Ma, D. Yang, Q.Li, K. Wang, B.Chen, J. F. Kennedy, J. Nie, Carbohydr. Polym. **79**(3), 620-627 (2010)
[3] J. D. Clapper; J. M. Skeie; R.F.Mullins; C.A.Guymon, Polymer., **48**(22), 6554-6564 (2007)

[4] T. Tashiro, Macromol. Mater. Eng., **286**(2), 63-87 (2001)
[5] Bio-inorganic Hybrid Nanomaterials: Strategies, Syntheses, Characterization and Applications, Editors: Eduardo Ruiz-Hitzky; Katsuhiko Ariga; Yuri M Lvov, Weinheim: Wiley-VCH, ISBN 978-3-527-31718-9 (2007)
[6] The supramolecular chemistry of organic-inorganic hybrid materials, Editors: Knut Rurack; Ramón Martínez-Máñez, Hoboken, N.J : Wiley, 2010, ISBN 978-0-470-37621-8
[7] Palmisano G, Le Bourhis E, Ciriminna R, Tranchida D, Pagliaro M, Langmuir, **22**(26), 11158–11162 (2006)
[8] W. J. Ho, C. J.Yuan, O Reiko, Anal. Chim. Acta, 572, 248-252 (2006)
[9] Melissinaki, A Gill, I. Ortega, M. Vamvakaki, A.Ranella, J.W. Haycock, C. Fotakis, M. Farsari, F. Claeyssens, Biofabrication **3**, 045005-045017 (2011)
[10] Sun M, Que W, Hub X, Opt. Mater., **32**, 49-53 (2009)
[11] Wang BL, Hu LL, Ceram Int,, **32**(1), 7-12 (2006)
[12] P. C. Rajath Varma, J. Colreavy, J. Cassidy, M. Oubaha, B. Duffy, C. McDonagh, Prog. Org. Coat., **66**, 406-411 (2009)
[13] A. Matei, M. Dinescu, E. C. Buruiana, T. Buruiana, I. Petcu, C. Mustaciosu, Dig. J. Nanomat. Biostruct., **6**(1), 29 (2011)
[14] B. K. Mann, J. L. West, Anat Rec **263,** 367–371 (2001)
[15] E. Stratakis, A. Ranella, M. Farsari, C. Fotakis, Prog. Quantum Electron **33,** 127 (2009)
[16] B. Lanfer, F.P. Seib, U. Freudenberg, D. Stamov, T. Bley, M. Bornhäuser, C.Werner, Biomaterials, **30,** 5950–5958 (2009)
[17] Yoon Sung Nam, Jun Jin Yoon, Tae Gwan Park, J. Biomed Mat Res, **3**(1), 1–7, (2000)
[18] B. Duan, W. L. Cheung, M. Wang, Biofabrication, **3**(1), 015001 (2011)
[19] S. D.Gittard, Narayan R. J., Expert Rev Med Devices, 7(3): 343–356 (2010)
[20] M. Malinauskas, P. Danilevičius, D. Baltriukienė, M. Rutkauskas, A. Žukauskas, Ž. Kairytė, G. Bičkauskaitė, V. Purlys, D. Paipulas, V. Bukelskienė, R. Gadonas, Lithuanian J. Phys., **50** (1), 75 (2010).
[21] M. Malinauskas, A. Žukauskas, V. Purlys, K. Belazaras, A. Momot, D. Paipulas, R. Gadonas, A. Piskarskas, H. Gilbergs, A. Gaidukeviciute, I. Sakellari, M. Farsari, S. Juodkazis, J. Opt. **12**, 124010 (2010)
[22] H. B. Sun, S. Kawata, Adv. Polym. Sci. **170**, 169 (2004)
[23] M. Farsari, M. Vamvakaki, B.N Chichkov, J. Opt. **12**, 124001 (2010)
[24] R. J. Narayan, C. Jin, A. Doraiswamy, I.N. Mihailescu, M. Jelinek, A. Ovsianikov, B.N. Chichkov, D. Chrisey, Adv. Eng. Mater., **7**(12), 1083 (2005)
[25] MR Prausnitz, Adv. Drug Deliv. Rev., **56**(5), 581 (2004)
[26] A. Ovsianikov, B. Chichkov, P.Mente, N.A. Monteiro-Riviere, A. Doraiswamy, R.J. Narayan, Int. J. Appl. Ceramic Technol., **4**(1), 22 (2007)
[27] R. Houbertz, P. Declerck, S. Passinger, A. Ovsianikov, J. Serbin, B.N. Chichkov, Phys. Stat. Sol. (a), **204**(11), 3662 (2007)
[28] A. Matei, M. Zamfirescu, F. Jipa, C. Luculescu, M. Dinescu, E.C.Buruiana, T. Buruiana, L.E.Sima, S.M.Petrescu, American Institute of Physics (AIP) proceedings, Melville, New York, **1278**: 843-851, (2010)
[29] A.Matei, M. Zamfirescu, C. Radu, M. Dinescu, E.C.Buruiana, T. Buruiana, L.E. Sima, S.M.Petrescu, Appl. Phys. A, **104** (3), 821-827 (2011)
[30] A.Tunçel, A. K. Özdemir, Z.Sümer, F.Hürmüzlü, Z.Polat, Dent. Mater. J. **25** (**2**), 267－271 (2006)